First Principles Study of Gallium Atom Adsorption on the α-Al_2O_3(0001) Surface

Rui Yang* and Alistair P. Rendell†

Department of Computer Science, College of Engineering and Computer Science, The Australian National University, Canberra, ACT 0200, Australia

Received: December 19, 2005; In Final Form: March 19, 2006

The adsorption of Ga atoms in low coverage on the Al-terminated α-Al_2O_3(0001) surface has been studied theoretically by using first principles periodic boundary condition (PBC) calculations within the framework of the generalized gradient approximation (GGA). Eight possible adsorption sites are investigated, but only two are found to correspond to stationary points. Both of these locations are characterized as hollow sites, with three surrounding surface O atoms and an Al atom in the center located deeper within the Al_2O_3 slab. The slight difference in the stability of these two sites is due to a difference in the chemical interactions between the Ga atom and the surface O atoms. Strong interactions between the Highest Occupied Molecular Orbital (HOMO) of the Ga atom and the surface state of the Al_2O_3 surface are observed. This interaction promotes charge transfer from the Ga to the surface Al atoms, which in turn causes the surface Al atoms to move up from the surface.

I. Introduction

Group III nitride semiconductors are of interest because of their applications in optical and electronic devices.[1,2] The preparation of bulk crystals of these nitrides is, however, rather difficult.[3] Normally these nitrides are grown heteroepitaxially on a suitable foreign substrate.[4] Of great concern in nitride research is the absence of a substrate with a lattice matching that of GaN. The most commonly used substrate is α-Al_2O_3 (sapphire) due to its fairly low price and because the α-Al_2O_3(0001) surface has a hexagonal pattern similar to the wurtzite structure of GaN(0001). Even then there is a 16% lattice mismatch between the α-Al_2O_3 and GaN and a 34% difference in their thermal expansion coefficients. To accommodate for this, and for differences in polarity, the relaxed rhombohedra surface of α-Al_2O_3 is transformed to a polar wurtzite structure, like AlN. This is accomplished by using a number of initial growth steps such as substrate surface cleaning, nitridation, and growth of a nucleation layer.[5]

X-ray photoelectron spectroscopy results have shown that an epitaxial-polished sapphire substrate is usually contaminated with hydrocarbon and fluorine atoms.[6,7] For example, hydrogen is found to be stable on the surface of Al_2O_3 even after annealing at 1100 °C under ultrahigh-vacuum conditions,[6] while carbon is found to be stable on an Al_2O_3 surface after annealing at 1100 K in an O_2 partial pressure of 5×10^6 Torr.[7] Although these impurities can normally be removed by using an O_2 or H_2/Ar plasma,[8] recent work by Davidsson et al. has suggested an alternative process that is based on the adsorption and evaporation of a layer of Ga atoms.[9] In this work Davidsson et al. used reflection high energy electron diffraction (RHEED) to investigate surface atomic periodicity and verified that a Ga cleaning process can remove impurities such as hydrocarbons and oxides from the Al_2O_3 surface. This offers a significant advantage in the preparation of GaN devices since it removes the need for an extra plasma source.

Ga cleaning has already been used on SiC substrates,[10] AlN buffer layers,[11] and GaN surfaces.[12−14] Despite this there have been very few detailed studies of this process. One exception is the work of Maffeis et al.,[14] who used soft X-ray photoelectron spectroscopy (SXPS) to study Ga adsorption on a GaN surface. They found that the adsorption produced a band-bending of 1.0 eV to high kinetic energy and re-vaporation of the deposited Ga resulted in a Fermi energy shift of 0.6 eV to lower energy. After the cleaning process, a Schottky barrier of height of 0.77 eV was observed.

The adsorption process for Ga on an Al_2O_3 surface might be expected to be similar to that of transition metals, especially those with a filled d-band such as Cu. For Cu atoms deposited on an Al_2O_3 surface it was reported that charge transfer occurs from the metal s-band to the Al_2O_3 slab.[15] Also, in a previous study we showed that adhesion at the Cu/α-Al_2O_3 (Al-terminated) interface comes mainly from electrostatic interactions and chemical bonding between Cu atoms and surface Al atoms.[16]

Ga does, however, have several different electronic properties compared to Cu, and as yet there appears to be no other theoretical studies of the adsorption of Ga on Al_2O_3. To address this deficiency we present in this paper a detailed theoretical investigation of the adsorption of Ga on a clean Al-terminated α-Al_2O_3(0001) surface. Several initial starting positions are considered, with the adsorption path for each analyzed. In all cases the Al_2O_3 surface was fully relaxed. In contrast with many other first principles computational studies in material science this work does not use a plane wave based method, but instead uses localized basis functions and a periodic supercell approach.[17−19]

II. Models and Computational Details

In the present work, the Ga atom adsorption on the Al terminated α-Al_2O_3(0001) surface was studied by using the quantum chemistry package, Gaussian 03.[20] The periodic boundary condition (PBC) method in Gaussian 03 allows simulation of surface phenomena by imposing periodicity only in two dimensions. This eliminates problems due to interactions between the surface and image surfaces that occur in calculations imposing periodicity in three dimensions.

The lattice constants of the bulk α-Al_2O_3 rhombohedra unit cell were determined by fitting energy−volume data to the

* Corresponding author. E-mail: rui.yang@anu.edu.au.
† E-mail: Alistair.Rendell@anu.edu.au.

10.1021/jp057391u CCC: $33.50
Published on Web 04/26/2006

TABLE 1: Comparison of the Crystal Lattice Constants of Al_2O_3 Bulk Obtained from Experiment with the Calculated Values Obtained with the LSDA/3-21g*, BLYP/3-21g*, and BLYP/6-31g* Methods

	exptl	LSDA/3-21g*	BLYP/3-21g*	BLYP/6-31g*
a_0 (Å)	5.128	5.039	5.180	5.226
error (%)		−1.73	+1.01	+1.91

TABLE 2: Change in the Interlayer Distance for the 18 Layer Al_2O_3 Model Slab Relative to Bulk Al_2O_3 Calculated with BLYP/3-21g* and BLYP/6-31g*, and in Comparison with Several Other Theoretical Results[a]

	Layers	BLYP/ 3-21g*	BLYP/ 6-31g*	ref 16	ref 28	ref 30	ref 31	ref 32
inner	O(2)−Al(4)	+7	+7	+7	+6	+4	+6	
	Al(3)−O(2)	+19	+22	+19	+22	+19	+19	+20
↓	Al(2)−Al(3)	−36	−36	−39	−49	−46	−42	−45
	O(1)−Al(2)	+2	+4	+2	+6	+3	+3	+3
surface	Al(1)−O(1)	−85	−84	−87	−86	−83	−87	−85

[a] Numbers given are percentages, with positive and negative values representing increases and decreases in the layer distance relative to the experimental bulk value, respectively.

Murnaghan equation of state.[21] Methods using both a local spin density approximation (LSDA) and a generalized gradient approximation (GGA) were considered, with results given in Table 1. These show that LSDA[22] gives the lowest value for the lattice constant, while the Becke−Lee−Yang−Parr (BLYP) GGA functional[23,24] gives a slight overestimate. This is typical for DFT calculations.[25] Although both methods give values that are in error by less than 2% compared to the experimental value, the BLYP functional was chosen for this work as it tends to provide better accuracy for bond energies.[26] It is noted that both the 3-21g* and 6-31g* basis sets give similar results for the Al_2O_3 crystal constants.

As a stoichiometric surface, the Al-terminated Al_2O_3(0001) surface is reported to be stable even at high oxygen partial pressure.[27−29] In this work a 1×1 Al-terminated α-Al_2O_3(0001) surface model was constructed and two-dimensional periodic boundary conditions imposed. To determine the minimum thickness necessary for the Al_2O_3 model slab, the surface energies where calculated for three slab thicknesses with 12, 18, and 24 layers (containing 4, 6, and 8 oxygen layers, respectively). With use of BLYP and a 6-31g* basis the surface energy for the 12-layer α-Al_2O_3(0001) model was calculated to be 1.41 J/m^2. This value changed to 1.47 J/m^2 for the 18-layer model, and then changed by just 0.01 J/m^2 when the model was further expanded to include 24 layers. Thus it was concluded that the 18-layer model was sufficient for the present work. We note that both the surface energy and the change in the surface energy with increasing surface layers obtained in this work agree well with previous GGA plane wave pseudopotential calculations[30] (where the surface energy changed from 1.50 J/m^2 for a 9-layer model to 1.59 J/m^2 for a 15−27 layer model).

Figure 1 shows the Al-terminated α-Al_2O_3 surface model with 18 layers. The top five surface layers dominate chemical bonding. These are plotted in progressively lighter shades of gray the further they are from the surface, and are explicitly labeled as Al(1), O(1), Al(2), Al(3), and O(2). For these layers Table 2 reports differences between the interlayer distances in the GGA optimized α-Al_2O_3 structure and the experimental values for bulk α-Al_2O_3. This shows that atoms in the outmost Al(1) layer move toward the O(1) layer below. The relaxed structure obtained with BLYP/3-21g* and BLYP/6-31g* calculations agrees well with our previous work performed using the plane-wave pseudopotential method,[16] and also with other first principles calculations.[28,30−32]

To our knowledge the adsorption of Ga on the Al_2O_3 surface has not been studied before with first principles methods. Thus as a first step we consider the adsorption behavior of a single Ga atom on the Al_2O_3 surface. For the 1×1 surface model used here this corresponds to 1/3 ML (monolayer) coverage. Eight possible initial positions were considered as starting points for the adsorption process. These eight sites are shown in Figure 1a and are similar to those used in other studies of hydrogen and copper adsorption on an Al_2O_3 surface,[15,29] except that some extra bridge positions are also considered. These initial positions are classified according to the type of atom under them. For example, Al_1, Al_2, and Al_3 positions lie above Al(1), Al(2), and Al(3) layer atoms, respectively. Similarly, O_1 and O_2 positions lie above O(1) and O(2) layer atoms, respectively.

From Table 2 it is apparent that due to the large relaxation of the Al(1) layer both the Al_1 and O_1 positions should be regarded as *on-top positions*, whereas Al_2, Al_3, and O_2 are *hollow positions*. If the stoichiometric Al_2O_3(0001) surface is divided into triangles with vertexes defined by the location of O(1) atoms, then there are four different types of triangles that are distinguished by the atom (from a lower layer) that resides at the center of that triangle. These triangles are shown in Figure 1b and will be referred to as the $O_{Al(1)}$, $O_{Al(2)}$, $O_{Al(3)}$, and $O_{O(2)}$ triangles accordingly. Between pairs of triangles there are three possible *bridge positions*, which we label as $B^{O(2)}_{Al(1)}$, $B^{O(2)}_{Al(2)}$, and $B^{O(2)}_{Al(3)}$ depending on which two O(2) triangles they connect.

At the beginning of each geometry optimization the Ga adsorbate was located at one of the points identified above and positioned 1.5 Å above the Al(1) layer. Only one side of the Al_2O_3 slab was deposited with Ga atoms.

The Berny algorithm developed by Schlegel et al.[33,34] and as implemented in Gaussian 03 was used to optimized the different initial structures. This algorithm uses the forces acting on the atoms together with an approximate second derivative or Hessian matrix to predict energetically more favorable structures, stopping when the forces go to zero. Symmetry constraints were not imposed. Since both BLYP/3-21g* and BLYP/6-31g* give reasonable structural properties for bulk and surface Al_2O_3, and in order to save computational time, initial structural optimizations were performed with BLYP/3-21g* which were then refined with BLYP/6-31g*.

III. Ga Adsorption Path on α-Al_2O_3(0001) Surface

Adsorption from all eight possible Ga starting positions relaxed to just two stationary points: one with the Ga atom sitting at the Al_3 position and another energetically less favorable structure with the Ga positioned at Al_2. To rigorously determine the nature of these stationary points (at least for this unit cell size) would require a frequency analysis to be performed. Unfortunately this is currently not possible as the PBC method in Gaussian 03 is yet to be extended to permit second derivative calculations. Given, however, that all eight starting locations relaxed to just two final structures, and that in both cases the Ga atom is located in a hollow position surrounded by Al(1) atoms, it seems highly unlikely that these stationary points are anything other than minima.

The adsorption energies at the Al_3 and Al_2 positions are −1.79 and −1.46 eV/atom, respectively (see Table 3). Upon adsorption of Ga the surface relaxation, shown in Figure 2, was found to be large. For both the Al_2 and Al_3 adsorbed Ga the surface Al(1) atoms moved away from the O(1) plane by ≈0.5 Å, with interlayer distance changes extending roughly 9 layers deep. Since, however, the opposite side of the slab is only slightly

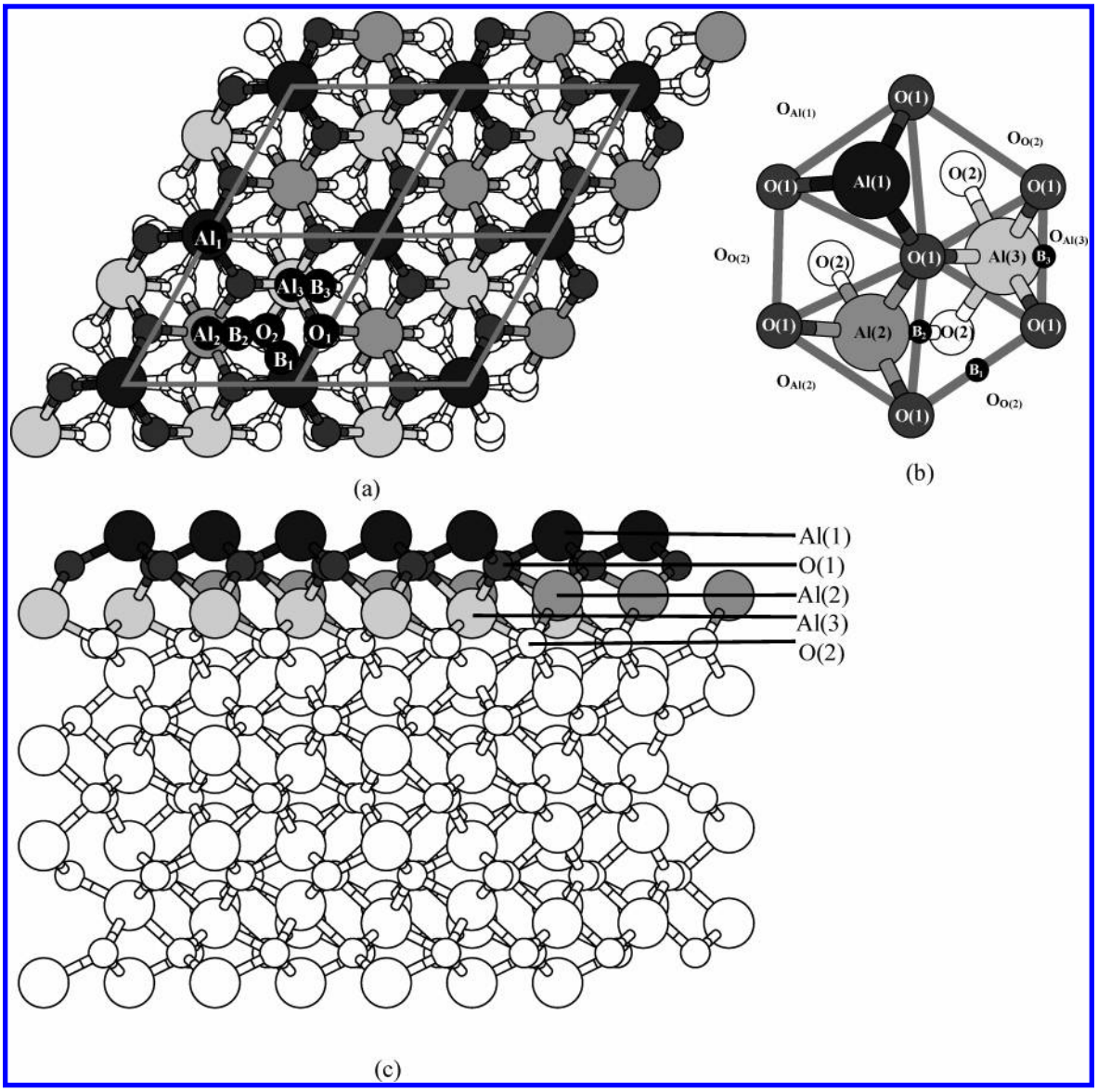

Figure 1. The 18 layer Al_2O_3 surface slab with larger circles used to indicate Al. (a) On-top view showing the 4 supercells and 8 initial adsorption positions within one of the supercells. (b) Surface view of a single supercell showing the 6 triangles defined by the locations of the O(1) atoms and distinguished by the central O(2), A1(1), A1(2), or A1(3) atom. Positions B_1, B_2, and B_3 correspond to the $B^{O(2)}_{Al(1)}$, $B^{O(2)}_{Al(2)}$ and $B^{O(2)}_{Al(3)}$ bridge positions, respectively. (c) The outmost five surface layers of the model slab showing the Al(1), O(1), Al(2), Al(3), and O(2) layers and with gray scale to characterize the distance from the surface.

TABLE 3: The Chemical (E^{Chem}_{ads}) and Structural (E^{Struct}_{ads}) Contributions to the Adsorption Energy (E^{total}_{ads}) Evaluated by Using BLYP/6-31g* Together with the Layer Distance between Ga and O(1) Layers for Ga Adsorbed at the Al_2 and Al_3 Sites[a]

favorite adsorption site	Al_2 site	Al_3 site
E^{total}_{ads} (eV/atom)	−1.46	−1.79
E^{Chem}_{ads} (eV/atom)	−2.18	−2.74
E^{Struct}_{ads} (eV/atom)	0.72	0.95
$d_{Ga-O(1)}$ (Å)	1.97	1.74
initial positions	Al_2, $B^{O(2)}_{Al(2)}$	Al_1, Al_3, O_1, O_2, $B^{O(2)}_{Al(1)}$, $B^{O(2)}_{Al(3)}$

[a] The initial starting positions for Al_2 and Al_3 site are also listed.

perturbed, it appears that the 18 layer model used in this work is thick enough.

It is of interest to explore briefly the paths taken during the optimization process for each of the eight initial Ga positions; although these paths are not guaranteed to be minimum energy paths they provide some indication of both the forces between the Ga atom and the Al/O atoms, and the extent to which the atomic layers within the Al_2O_3 are distorted, as the Ga moves over the Al_2O_3 surface. This information is summarized in Figure 3a−h. For each of the panels the left-hand side shows the planar displacement of the Ga and Al(1) atoms, changes in the Ga−O(1) and Al(1)−O(1) interlayer distance, and the total system energy as a function of optimization step. The right-hand side shows the path taken by the Ga atom over the Al_2O_3 surface. We now consider the key features of each optimization path according to the nature of the initial adsorption site.

A. Hollow Positions. From the Al_2 (Figure 3a) and Al_3 (Figure 3b) starting positions the main structural change is an adjustment in the height of the Ga atom above the O(1) plane. Accompanying this movement, the outmost Al(1) atoms move away from the O(1) surface. For example, the Al(1)−O(1) distance changes from 0.13 Å for the α-Al_2O_3 free surface to 0.558 and 0.624 Å when Ga is adsorbed at either the Al_2 or Al_3 site, respectively. Similar displacements of Al(1) atoms are also

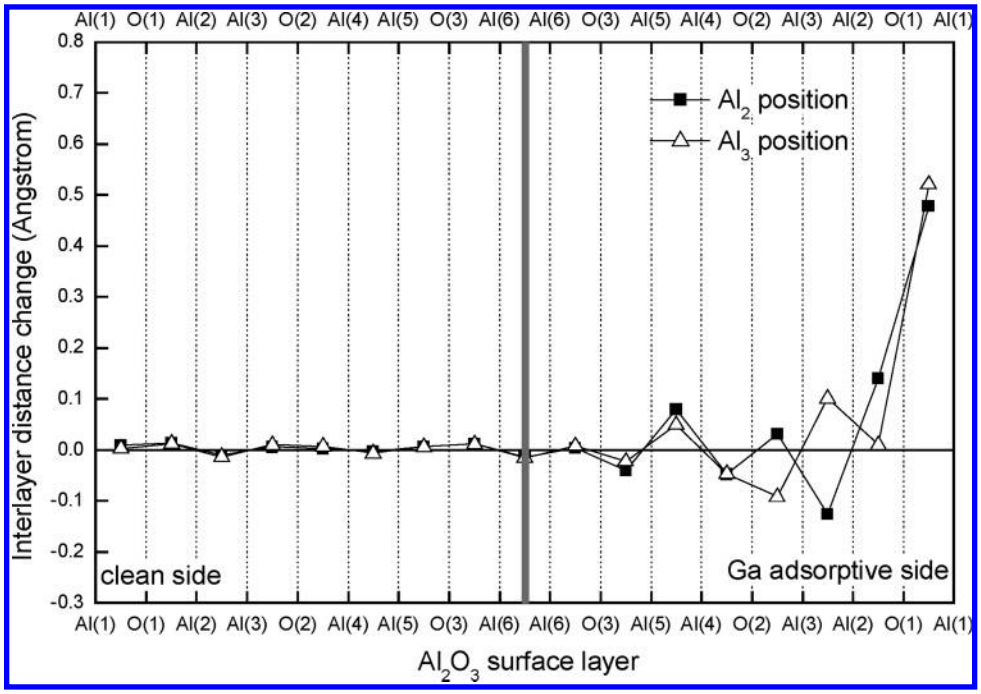

Figure 2. The interlayer distance changes of Ga adsorbed on the Al_2O_3 surface at the Al_2 and Al_3 positions and relative to the Al_2O_3 free surface. The middle of the slab is indicated by the solid vertical line.

found when Cu or Pd are adsorbed on an α-Al_2O_3 surface[15,29] and also at the Cu/α-Al_2O_3 interface.[16] Such a displacement is indicative of a weakening of the outermost Al(1) to O(1) bond. Since Al_2O_3 is essentially an ionic solid, this weakening equates to a reduction in the ionicity of the surface aluminum ions. As will be discussed in Section V, this is due to charge transfer from the Ga atom to the Al_2O_3 surface, and particularly onto the surface Al(1) atoms.

From the O_2 starting position the Ga atom moves to the neighboring hollow Al_3 position as shown in Figure 3c. The relaxation process can be divided into two stages: stage A when the Ga atom lies within the $O_{O(2)}$ triangle, and stage B when it moves into the $O_{Al(3)}$ triangle. In stage A the Ga atom first moves directly away from the nearby Al(1) atom. This is indicative of the Ga atom losing charge to the Al_2O_3 slab, becoming slightly positively charged, and as a result being repelled away from the (positively charged) Al(1) atom. Having moved away from its initial position the Ga atom then moves to the bridge site connecting the $O_{O(2)}$ and $O_{Al(3)}$ triangles before finally arriving at the Al_3 position.

B. On-Top Positions. From the O_1 on-top position (Figure 3d) the Ga atom again moves in a direction away from the nearby Al(1) atom before relaxing toward the Al_3 position. In this case the Al(1) atoms leave the O(1) plane at the very beginning of the optimization process.

From the Al_1 on-top position (Figure 3e) the Ga atom has to pass through an $O_{O(2)}$ triangle to arrive at either the Al_2 or Al_3 positions. As before the relaxation process can be divided into a number of stages depending on which triangle the Ga atom is located in. These are marked as A, B, and C in Figure 3e. In the first stage the Ga atom stays at the Al_1 position and adjusts its height according to the bonding between Ga and the Al(1) atom. In the second stage the Ga atom moves to the neighboring O_2 hollow position. While in the third stage the Ga atom moves from the O_2 site to the Al_3 site in a manner similar to that observed when starting from the O_2 position (i.e., similar to that shown in Figure 3c). It is noted that changes in the Al(1) to O(1) interlayer separation are suppressed in stages A and B, with the majority of this movement taking place in stage C after the Ga atom has moved some distance away from the starting Al_1 position.

C. Bridge Positions. From the results obtained above it is already apparent that the two bridge positions $B^{O(2)}_{Al(2)}$ and $B^{O(2)}_{Al(3)}$ will move to the Al_2 and Al_3 positions, respectively. This is confirmed in Figure 3f,g. In both cases a significant increase in the Al(1)−O(1) separation occurs at the beginning of the adsorption process.

From the $B^{O(2)}_{Al(1)}$ bridge position, the Ga atom first moves to the O_2 position before turning and moving toward the Al_3 position (Figure 3h). In this case it appears that the repulsive interaction between Al(1) and Ga atoms is large enough to suppress outward relaxation of Al(1) atoms until after the Ga atom has reached the O_2 position. From the O_2 position the Ga atom relaxes to the final Al_3 position in a manner similar to that observed in Figure 3c.

In summary, there appears to be just two possible adsorption positions for Ga atoms on the Al_2O_3(0001) surface: the Al_3 position and the energetically less favorable Al_2 position. Of the eight Ga starting positions considered here two optimize to the Al_2 position, while the other six all optimize to the Al_3 position. This is true even though in some cases the Ga atom had to move a long distance to arrive at the final Al_3 position. Except for cases where the Ga atom was initially located close to the Al_2 or Al_3 position, all optimizations were characterized by an initial phase in which the Ga atom was repulsed away from the surface Al(1) atom. A charge transfer from the Ga to the Al(1) atom appears to occur at the beginning of each adsorption process.

IV. Adsorption Energy

To explore the different chemical and structural contributions to the adsorption energy, we adopt the same scheme as used in our previous study of segregation effects on cohesion at the Fe

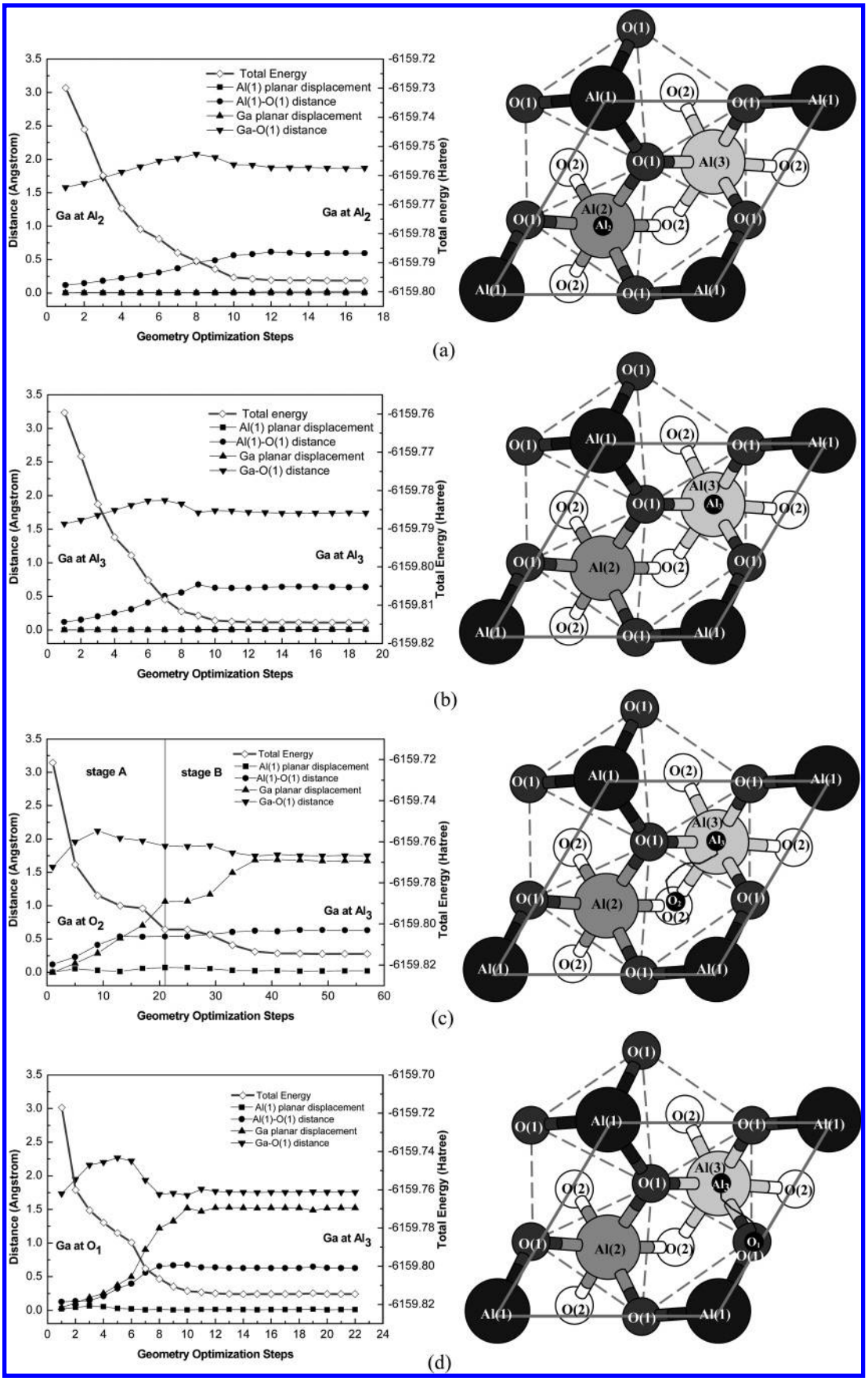
Total Energy
Al(1) planar displacement
Al(1)-O(1) distance
Ga planar displacement
Ga-O(1) distance
Distance (Angstrom)
Total energy (Hatree)
Geometry Optimization Steps
Ga at Al2
Ga at Al3
Ga at O2
Ga at O1
stage A
stage B
(a)
(b)
(c)
(d)

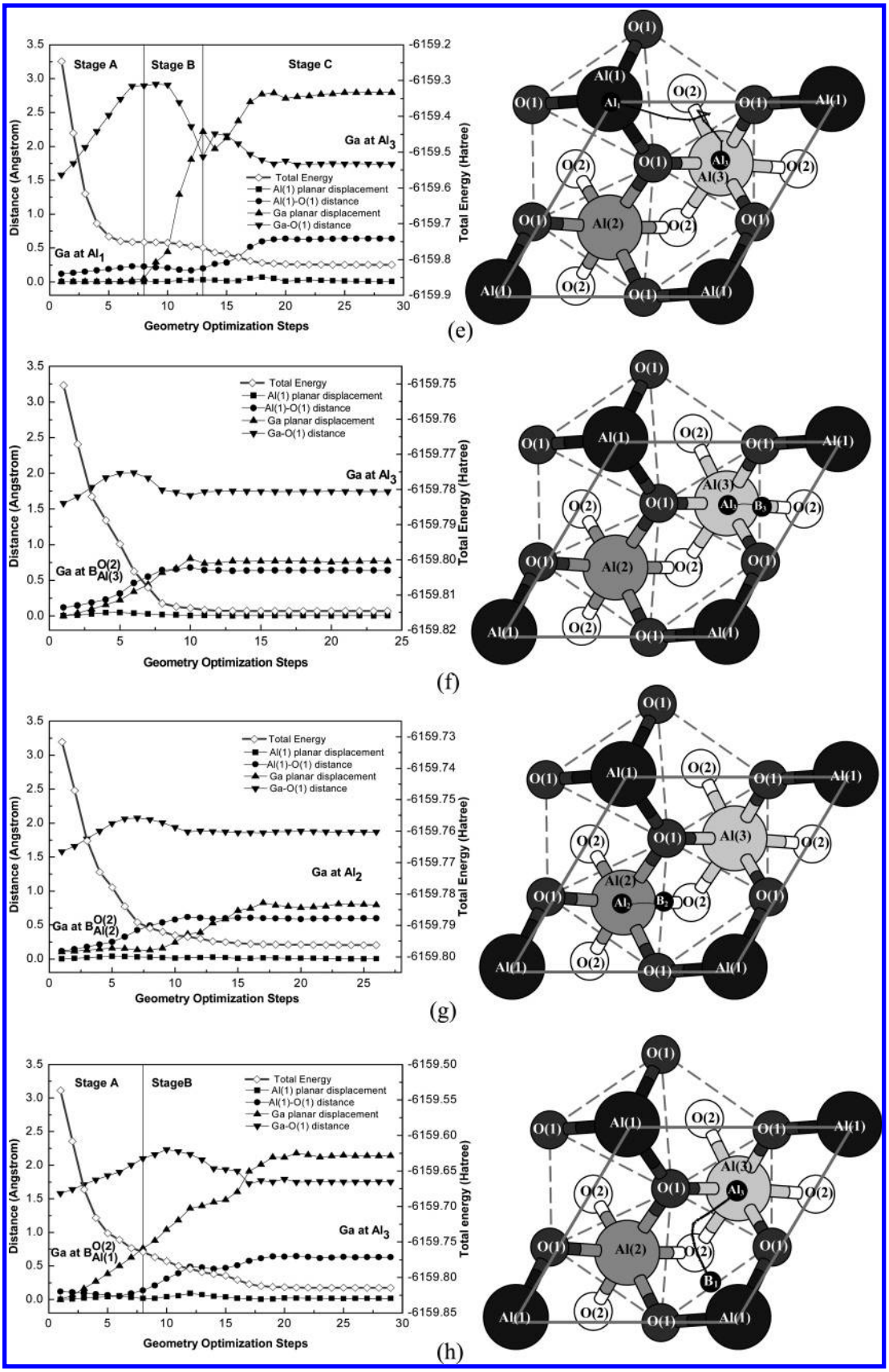

Figure 3. In-plane displacement of the Ga and Al(1) atoms from their initial positions together with the changes in the Ga−O(1) and Al(1)−O(1) vertical separation for Ga adsorption at the (a) Al_2, (b) Al_3, (c) O_2, (d) O_1, (e) Al_1, (f) $B^{O(2)}_{Al(3)}$, (g) $B^{O(2)}_{Al(2)}$, and (h) $B^{O(2)}_{Al(1)}$ positions as a function of geometry optimization step. The total energies for each system are also shown on the right hand axis of each diagram. The diagram on the right-hand side shows the path taken by the Ga atom over the Al_2O_3 surface during the course of the geometry optimization.

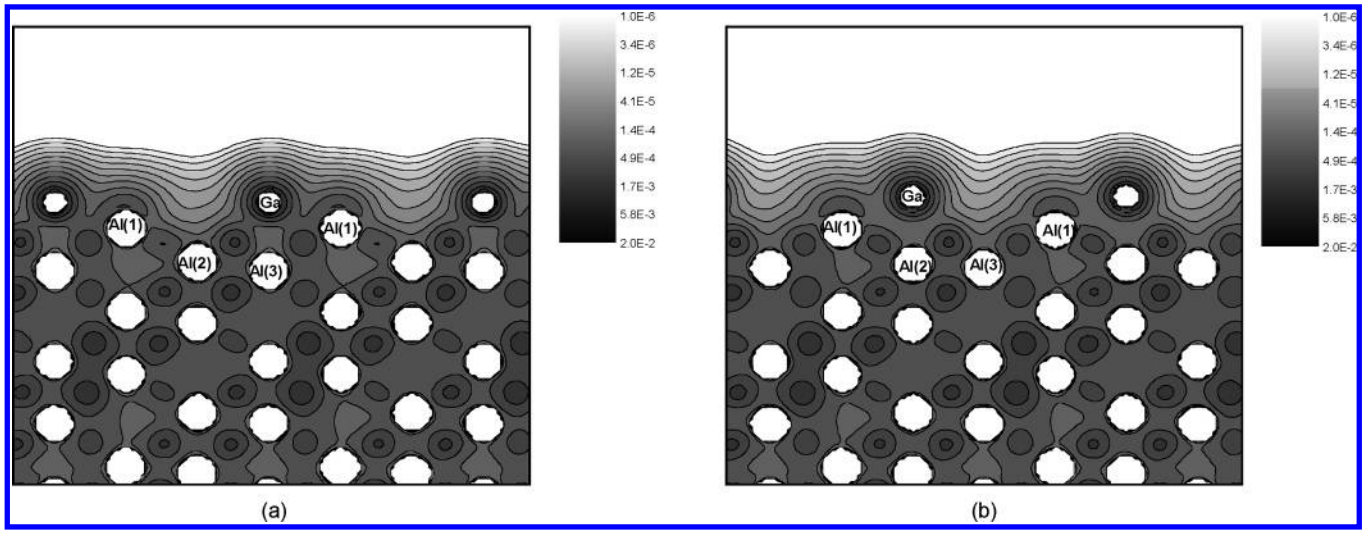

Figure 4. The charge density of the Al_2O_3 surface for Ga adsorbed at the (a) Al_3 and (b) Al_2 positions.

grain boundary.[35] In this scheme the adsorption energy of Ga on the Al_2O_3 surface is divided into two stages:

$$\begin{matrix}\text{isolated Ga} + \\ \text{Al}_2\text{O}_3\text{ free surface}\end{matrix} \xrightarrow{\text{stage1}} \begin{matrix}\text{isolated Ga} + \\ \text{isolated Al}_2\text{O}_3\text{ surface}\end{matrix} \xrightarrow{\text{stage 2}} \begin{matrix}\text{Ga adsorbed on} \\ \text{Al}_2\text{O}_3\text{ surface}\end{matrix}$$

The first stage involves structural changes from the Al_2O_3 free surface to an isolated Al_2O_3 surface that has the same structural configuration as found in the optimized Ga adsorbed Al_2O_3 system. The energy change for this stage represents a structural contribution to the adsorption energy and is denoted as E_{ads}^{Struct}. The second stage concerns only chemical bond formation between the Ga adsorbate and the structurally prepared Al_2O_3 surface. This stage represents the chemical contribution to the adsorption energy and is denoted as E_{ads}^{Chem}. The total adsorption energy consists of both contributions, i.e., $E_{ads}^{total} = E_{ads}^{Struct} + E_{ads}^{Chem}$.

As listed in Table 3, E_{ads}^{Struct} for Ga at the Al_3 position is 0.95 eV, which is comparable but somewhat larger than that for Ga at the Al_2 position (0.72 eV). The distance between the adsorbed Ga and the O(1) plane at the Al_3 position is 1.74 Å, which is less than the 1.97 Å for the Al_2 position. From this it might be expected that a Ga atom sitting at the Al_3 position will cause greater changes in the α-Al_2O_3 surface compared to one sitting at the Al_2 position.

The chemical contributions to the adsorption energies (E_{ads}^{Chem}) are quite different at -2.74 eV for Ga at the Al_3 position compared to -2.18 eV for Ga at the Al_2 position. The calculated valence electron density plots are given in Figure 4 and provide some insight into the bonding differences at these two sites. Notably the charge density around the Ga and neighboring O(1) atoms shown in Figure 4a for the Al_3 adsorbed Ga is greater than that for the Al_2 adsorbed Ga shown in Figure 4b. Thus the O(1) atoms form stronger interactions with a Ga atom sitting at the Al_3 position compared to one sitting at the Al_2 position. A detailed chemical bonding analysis of Ga−O interaction will be given in Section V.

V. Chemical Bonding and Electronic Structure

Figure 4 shows that there is a slight charge accumulation above the Al(1) atoms regardless of whether the Ga atom is located at the Al_2 or Al_3 position. Such a charge accumulation has been found in many metal and ionic oxide ceramic systems, and is regarded as polarization of the metal atoms due to the oxide surface electrostatic field.[15,36−38] Alternatively for Al_2O_3, this charge buildup can also be interpreted as a movement of charge into the Al−surface dangling bond. To investigate this further we have computed density-of-state (DOS) curves and molecular orbital maps. In Figures 5 and 6 the DOS of the isolated Ga, the isolated Al_2O_3 surface, and the Ga adsorbed Al_2O_3 system are plotted on the left-hand sides for Ga adsorbed at the Al_3 and Al_2 sites, respectively. The right-hand side of each figure gives the real space distribution of either the corresponding HOMO or LUMO. Examination of the DOS curves clearly shows the insulator character of the isolated Al_2O_3 substrate, but an almost metallic character when the Ga atom is adsorbed. The HOMO in the α band of the Ga atom consists mainly of s and p_z orbitals according to the real space distribution shown in Figure 5a. It is noted that the LUMO of the isolated Al_2O_3 surface lies within the band gap and mainly comes from the Al(1) p_z dangling orbital as shown by the real space distribution plotted in Figure 5b. Such a surface state seems common for the Al_2O_3 surface and has been found in another study using periodic Hartree−Fock theory[39] and also in our pervious study of the Cu/Al_2O_3 interface that used a plane-wave pseudopotential method.[40] In the present work, the HOMO of the Ga atom and the LUMO of the isolated Al_2O_3 system have similar energies that largely overlap in real space. These combine to form the HOMO orbital of the Ga adsorbed Al_2O_3 system, shown in Figure 5c for the Al_3 positioned Ga and in Figure 6c for the Al_2 positioned Ga, with relatively little distortion. This suggests that the HOMO has little (if any) covalent bonding character, rather that the Ga−Al interaction is more metallic in nature.

The charge redistribution that occurs between the Ga HOMO and the Al_2O_3 LUMO is shown in Figure 7a,b. These are calculated according to the charge difference, $\Delta\rho$, where $\Delta\rho = \rho(Ga/Al_2O_3) - \rho(Al_2O_3\text{ surface}) - \rho(Ga\text{ atom})$, and are plotted along the diagonal plane of the supercell containing the Al(1), Al(2), Al(3), and Ga atoms. A clear gain of electron density appears in the region around the surface Al(1) atoms, while there is a decrease in charge density around the Ga atom for both the Al_3 and Al_2 adsorbed Ga. The decreased charge density surrounding the Ga atom on the side opposite to the Al(1) atoms gives further evidence of charge transfer from the Ga to the Al(1) atoms. This charge transfer arises from bonding interactions between the HOMO of the Ga atom and the surface state

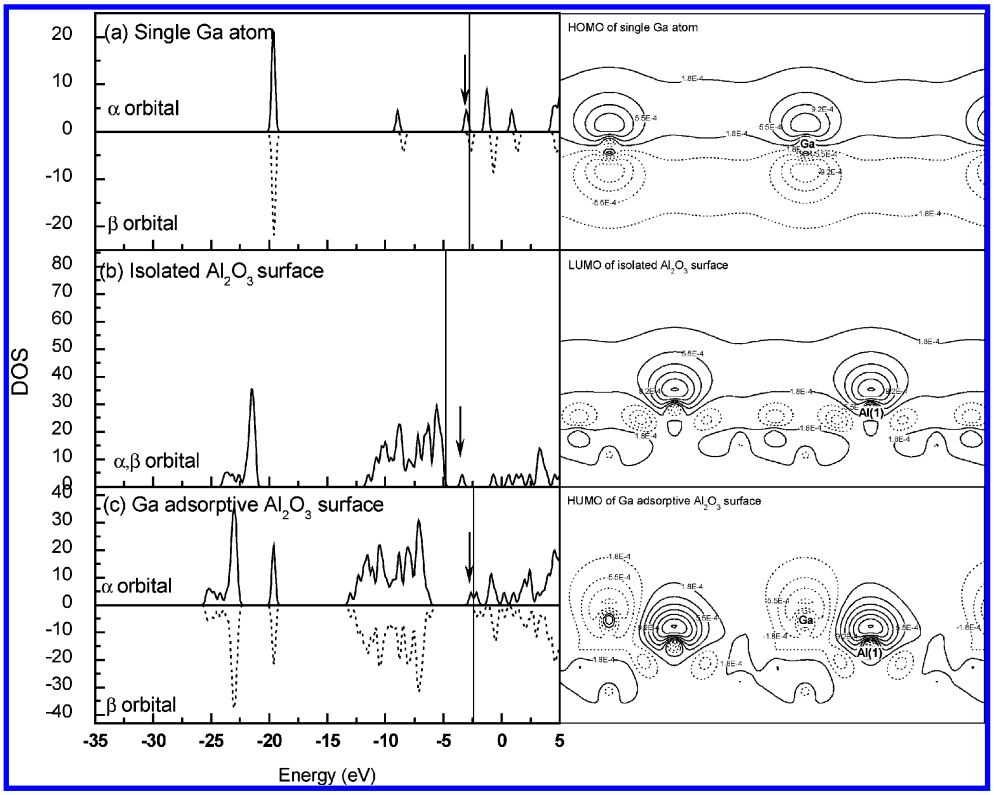

Figure 5. DOS curves and the real space distribution of the HOMO or LUMO of (a) the Ga atom, (b) the isolated Al_2O_3 surface slab, and (c) the Ga adsorption Al_2O_3 surface with Ga sitting at the Al_3 position. The Fermi energy levels are represented as the vertical line in each diagram. The vertical downward arrow indicates the energy level of the HOMO or LUMO of each system.

of the isolated Al_2O_3. Such a charge-transfer interaction mechanism was also observed in our previous study of the Cu/Al_2O_3 interface.[40] However, the extended metal-induced gap state (MIGS) of Cu makes it difficult to find bonding partners for the Cu band interacting with the Al_2O_3 surface state. In the present work, the LUMO of the Ga atom has a discrete energy level, which gives a clearer picture of the bonding process with the surface state of the Al_2O_3 slab.

To explore the nature of the Ga−O bonding the charge redistributions on planes defined by either the Al(2) or Al(3) atom, an adjacent O(1) atom and the adsorbed Ga atom are plotted in Figure 8a,b for the Al_3 and Al_2 positions, respectively. These show a depletion of charge from the O(1) layer and a corresponding increase in charge around the Ga atom. Such charge polarization can be attributed to the positively charged Ga atom depleting electron density from the oxygen atoms in the O(1) layer. Moreover, since the distance between the adsorbed Ga and the O(1) plane is smaller at the Al_3 position (1.74 Å) compared to that at the Al_2 position (1.97 Å) we might expect this effect to be larger at the Al_3 position; inspection of Figure 8a,b shows this is indeed the case.

VI. Discussion

The surface state of the α-Al_2O_3(0001) slab seems sensitive to the interlayer distance between the Al(1) and O(1) planes. For the α-Al_2O_3 free surface where the Al(1)−O(1) interlayer distance is 0.13 Å, the surface state lies at the bottom of the conduction band as shown in Figure 9a. For the isolated α-Al_2O_3 structure used to evaluate E_{ads}^{Struct} the Al(1)−O(1) interlayer distance is significantly larger at 0.558 Å for the Al_2 adsorbed Ga structure and 0.624 Å for the Al_3 adsorbed Ga structure. Plots of the density of states for these two systems are shown in Figure 9. These show that in both cases the surface state shifts substantially to lower energy.

As the spatial range of this surface state extends over the entire surface (as shown on the right-hand side of Figure 5b,c) it can interact with a Ga atom lying at any initial position on the surface. Reaction between the α-Al_2O_3 surface state and Ga HOMO results in a charge transfer from the Ga atom to the Al(1) atom. This is evident from the charge buildup around the Ga nuclei in Figure 7a,b, and an increase in the Al(1)−O(1) interlayer separation.

Adsorption of Ga onto the α-Al_2O_3 surface appears to proceed via an initial interaction between the Ga HOMO and the α-Al_2O_3 LUMO. This reaction, albeit weak initially due to the relatively high energy of the α-Al_2O_3 LUMO (Figure 8a), is sufficient to result in some charge transfer from the Ga atom to the Al(1) atoms. This charge transfer weakens the electrostatic interaction between the Al(1) and O(1) atoms causing the interlayer separation between these two layers to increase. This in turn lowers the energy of the Al_2O_3 LUMO resulting in more charge transfer that increases the Al(1) to O(1) separation even further. The only exception to this positive feedback is when the Ga atom is initially positioned close to the Al(1) atom. In this case increases in the Al(1) to O(1) separation are limited until the Ga atom has moved away from the Al(1) atom, but this appears to occur quite quickly as charge transfer has made the Ga slightly positive causing it to be repulsed away from the positive Al(1) atom.

The positive Ga atom, while repulsed away from the Al(1) atoms, is now attracted toward the negatively charged O(1) atoms. There are only two viable adsoption sites that balance the repulsive interactions from the surrounding Al(1) atoms with the bonding interaction from the O(1) atoms, namely the Al_2 and Al_3 positions. These sites are at the common centers of two surface triangles defined by the locations of either Al(1) atoms or O(1) atoms.

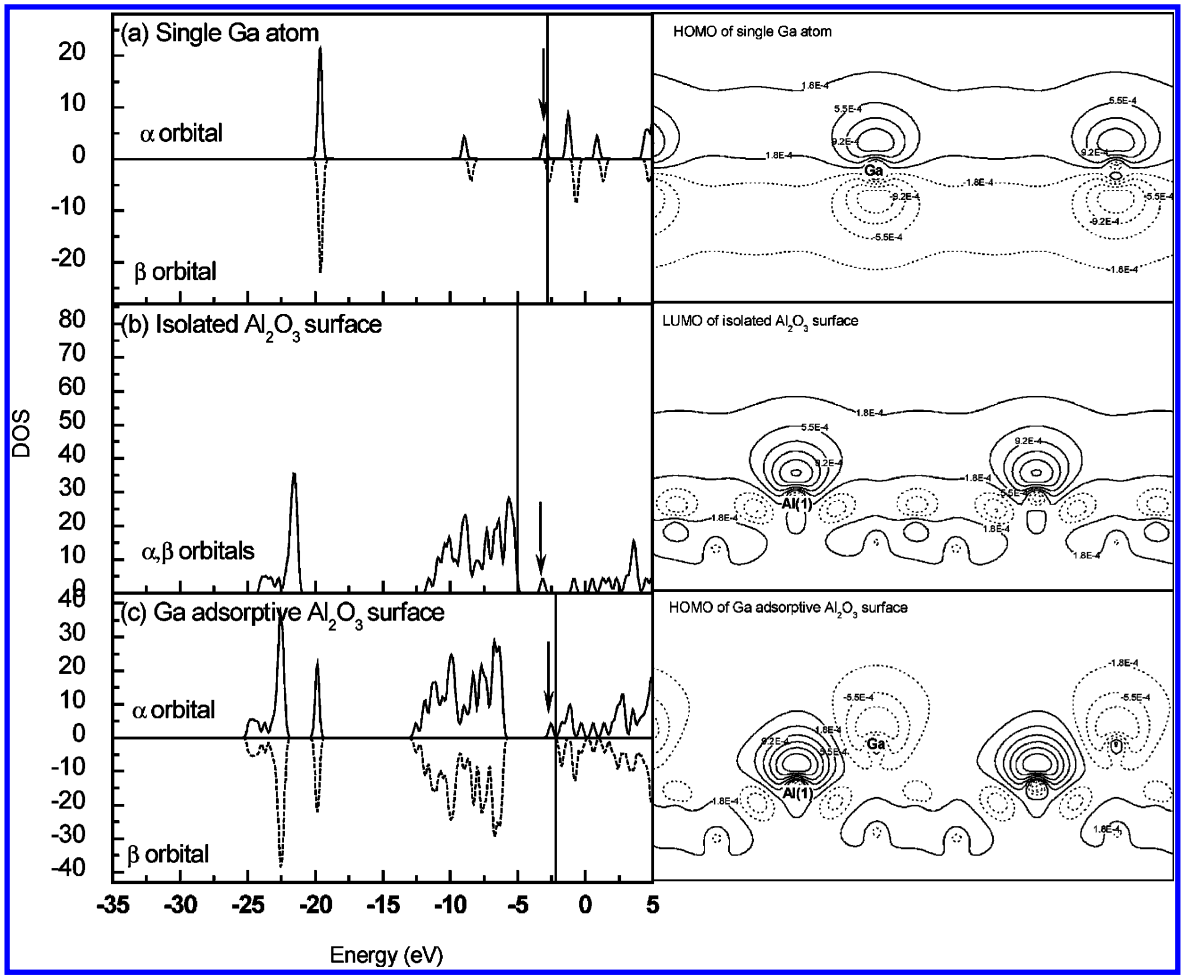

Figure 6. DOS curves and the real space distribution of the HOMO or LUMO of (a) the Ga atom, (b) the isolated Al_2O_3 surface slab, and (c) the Ga adsorption Al_2O_3 surface with Ga sitting at the Al_2 position. The Fermi energy levels are represented as the vertical line in each diagram. The vertical downward arrow indicates the energy level of the HOMO or LUMO of each system.

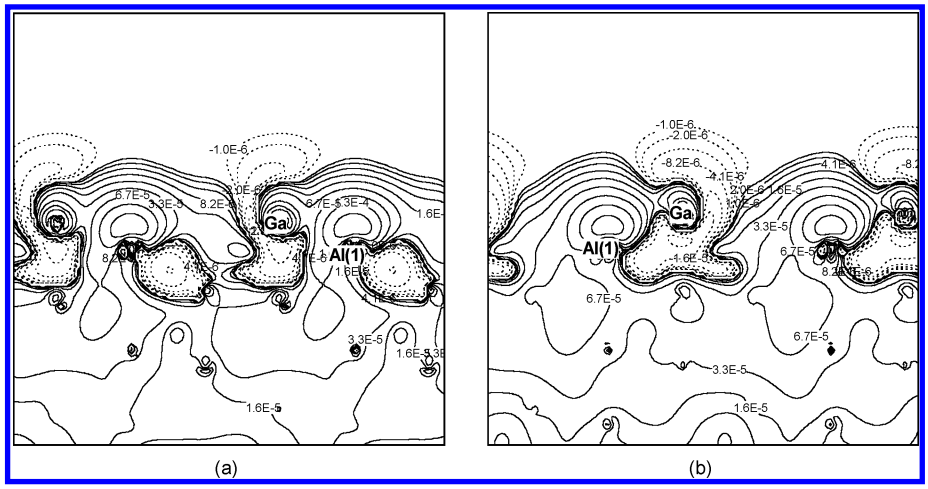

Figure 7. Charge redistribution evaluated on a diagonal plane containing Al(1), Al(2), and Al(3) atoms for the Ga atom sitting at the (a) Al_3 and (b) Al_2 positions. Positive contours (solid lines) denote charge accumulation due to Ga adsorption and negative contours (dotted lines) denote charge depletion.

It should be stressed that the results here relate to 1/3 ML Ga coverage, and if coverage is increased beyond this the relative stability of the different adsorption sites could change. Such coverage dependence has been observed for other metal/Al_2O_3 systems. For example, Verdozzi et al.[31] found that at 1/3 ML coverage Pt atoms prefer to occupy the O_1 position on the Al_2O_3 surface, but at 1 ML coverage they prefer the Al_1 position. A similar dependence was also found for the Pd/Al_2O_3 system, where the O_1 position is preferred at 1/3 ML coverage but the Al_1 position is preferred at 1 ML coverage.[37] Work is currently underway to study this aspect of the Ga/Al_2O_3 system.

In contrast to the results reported here the most stable site for an H atom on the Al_2O_3 surface is the Al_1 site.[28] This difference is probably not surprising—given that H has just one electron it will be attracted to the most positive site on the surface. Removal of hydrogen with use of a 1/3 ML Ga cleaning

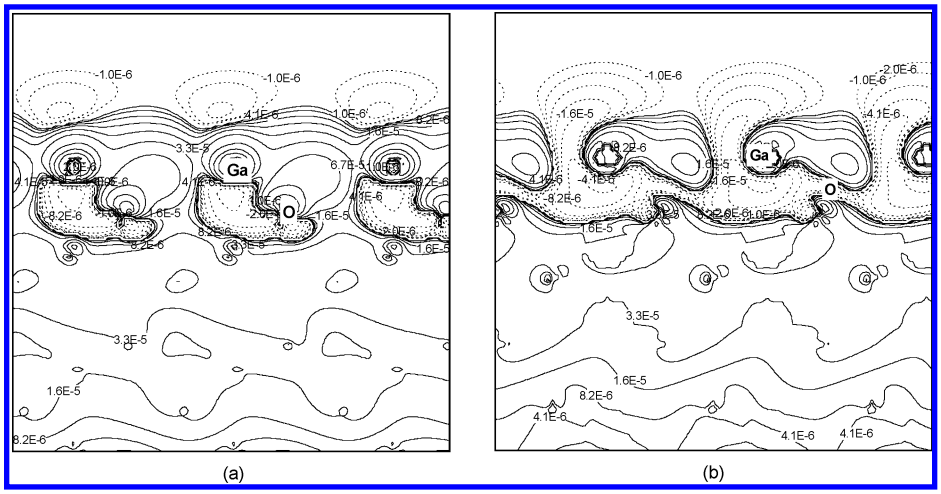

Figure 8. Charge redistribution evaluated on a plane defined by either the Al(2) or Al(3) atom, an adjacent O(1) atom, and the adsorbed Ga atom for the case of (a) Al_3 and (b) Al_2 positions. Positive contours (solid lines) denote charge accumulation and negative contours (dotted lines) denote charge depletion.

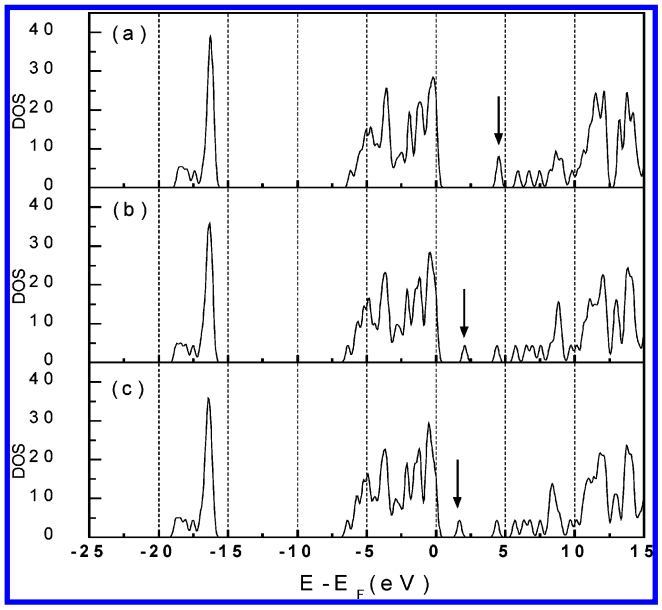

Figure 9. The DOS curves for (a) the Al_2O_3 free surface, (b) the isolated Al_2O_3 surface after Ga is removed from the Al_2 position, and (c) the isolated Al_2O_3 surface after Ga is removed from the Al_3 position. The vertical downward arrows indicate the energy level of the HOMO of each system.

process probably proceeds by formation of a Ga/H surface complex, that has less adhesion to the slab and can easily be removed by annealing. With increased coverage the Ga atom will, however, began to compete with the hydrogen atom to occupy the Al_1 position.

VII. Conclusions

In the present work, the adsorption of Ga at 1/3 ML coverage on an Al-terminated α-Al_2O_3(0001) surface has been studied by using a first principles 2D periodic supercell approach. Evidence was found for charge transfer from the Ga atoms to the Al_2O_3 surface, and specifically to the outmost Al atoms. This appears to result from interaction between the Ga HOMO and the surface state of the Al_2O_3 slab. As a consequence of this charge transfer the electrostatic bond between the outmost Al atoms and their neighboring O atom is weakened causing the Al atoms to move significantly out from the surface.

Although eight possible binding sites were considered, only two were found to correspond to stationary points. These two sites are characterized by three surrounding surface O atoms that form a triangle, and an Al atom that is located at the center of the O triangle but at a lower level in the Al_2O_3 slab. Of these two possible "*hollow*" sites the one with the Al located deeper within the Al_2O_3 slab is found to be more stable.

Acknowledgment. This work is funded by Australian Research Council Linkage Grant LP0347178 and is in association with Gaussian Inc. and Sun Microsystems. Provision of computer time from the Australian Partnership in Advanced Computing is gratefully acknowledged, as is the donation of computing resources from Alexander Technology.

References and Notes

(1) Nakamura, S.; Senoh, M.; Mukai, T. *Appl. Phys. Lett.* **1993**, *62*, 2390.
(2) Khan, M. A.; Kuznia, J.; Olson, D.; Schaff, W.; Burm, J.; Shur, M. *Appl. Phys. Lett.* **1994**, *65*, 1121.
(3) Teisseyre, H.; Leszczybski, M.; Suski, T.; Grzegory, I.; Bockowski, M.; Jun, J.; Porowski, S.; Pakula, K.; Robert, J. L.; Beaumont, B.; Gibart, P.; Vaille, M.; Faurie, J. P. *Semicond. Sci. Technol.* **1997**, *12*, 240.
(4) Jain, S. C.; Willander, M.; Narayan, J.; Overstraeten, R. V. *J. Appl. Phys.* **2000**, *87*, 965.
(5) Seelmann-Eggebert, M.; Zimmermann, H.; Obloh, H.; Niebuhr, R.; Wachtendorf, B. *J. Vac. Sci. Technol. A* **1998**, *16*, 2008.
(6) Ahn, J.; Rabalais, J. W. *Surf. Sci.* **1997**, *388*, 121.
(7) Niu, C.; Shepherd, K.; Martini, D.; Tong, J.; Kelber, J. A.; Jennison, D. R.; Bogicevic A. *Surf. Sci.* **2000**, *465*, 163.
(8) Namkoong, G.; Doolittle, W. A.; Brown, A. S.; Losurdo, M.; Capezzuto, P.; Bruno, G. *J. Appl. Phys.* **2002**, *91*, 2499.
(9) Davidsson, S. K.; Andersson, T. G.; Zirath, H. *Appl. Phys. Lett.* **2002**, *81*, 664.
(10) Ploog, K.; Brandt, O.; Muralidharan, R.; Thamm, A.; Waltereit, P. *J. Vac. Sci. Technol. B* **2000**, *18*, 2290.
(11) Khan, M. A.; Kuznia, J. N.; Olson, D. T. *J. Appl. Phys.* **1993**, *73*, 3108.
(12) Bermudez, V. M.; Kaplan, R.; Khan M. A.; Kuznia, J. N. *Phys. Rev. B* **1993**, *48*, 2436.
(13) Kampen, T. U.; Mönch, W. *Appl. Surf. Sci.* **1997**, *117/118*, 388.
(14) Maffeis, T.; Clark, D.; Dunstan, P.; Wilks, S.; Evas, D.; Peiro, F.; Riechert, H.; Parbrook, P. *Phys. Status Solidi A* **1999**, *176*, 751.
(15) Hernandez, N. C.; Sanz, J. F. *J. Phys. Chem. B* **2002**, *106*, 11495.
(16) Yang, R.; Tanaka, S.; Kohyama, M. *Philos. Mag.* **2005**, *85*, 2961.
(17) Kudin, K. N.; Scuseria, G. E. *Chem. Phys. Lett.* **1998**, *289*, 611.
(18) Kudin, K. N.; Scuseria, G. E. *Chem. Phys. Lett.* **1998**, *283*, 61.
(19) Kudin, K. N.; Scuseria, G. E. *Phys. Rev. B* **2000**, *61*, 16440.
(20) Frisch, M. J.; Trucks, G. W.; Schlegel, H. B.; Scuseria, G. E.; Robb, M. A.; Cheeseman, J. R.; Montgomery, J. A., Jr.; Vreven, T.; Kudin, K. N.; Burant, J. C.; Millam, J. M.; Iyengar, S. S.; Tomasi, J.; Barone, V.; Mennucci, B.; Cossi, M.; Scalmani, G.; Rega, N.; Petersson, G. A.; Nakatsuji, H.; Hada, M.; Ehara, M.; Toyota, K.; Fukuda, R.; Hasegawa, J.; Ishida, M.; Nakajima, T.; Honda, Y.; Kitao, O.; Nakai, H.; Klene, M.; Li, X.; Knox, J. E.; Hratchian, H. P.; Cross, J. B.; Adamo, C.; Jaramillo, J.;

Gomperts, R.; Stratmann, R. E.; Yazyev, O.; Austin, A. J.; Cammi, R.; Pomelli, C.; Ochterski, J. W.; Ayala, P. Y.; Morokuma, K.; Voth, G. A.; Salvador, P.; Dannenberg, J.; Zakrzewski, V. G.; Dapprich, S.; Daniels, A. D.; Strain, M. C.; Farkas, O.; Malick, D. K.; Rabuck, A. D.; Raghavachari, K.; Foresman, J. B.; Ortiz, J. V.; Cui, Q.; Baboul, A. G.; Clifford, S.; Cioslowski, J.; Stefanov, B. B.; Liu, G.; Liashenko, A.; Piskorz, P.; Komaromi, I.; Martin, R. L.; Fox, D. J.; Keith, T.; Al-Laham, M. A.; Peng, C. Y.; Nanayakkara, A.; Challacombe, M.; Gill, P. M. W.; Johnson, B.; Chen, W.; Wong, M. W.; Gonzalez, C.; Pople, J. A. *Gaussian 03*, Revision C.02; Gaussian, Inc.: Wallingford, CT, 2004.

(21) Murnaghan, F. D. *Proc. Natl. Acad. Sci.* **1944**, *30*, 244.

(22) Vosko, S. H.; Wilk, L.; Nusair, M. *Can. J. Phys.* **1980**, *58*, 1200.

(23) Becke, A. D. *Phys. Rev. A* **1988**, *38*, 3098.

(24) Lee, C.; Yang, W.; Parr. R. *Phys Rev. B* **1988**, *37*, 785.

(25) Khein, A.; Singh, D. J.; Umrigar, C. J. *Phys. Rev. B* **1995**, *51*, 4105.

(26) Johnson, B. G.; Gill. P. M. W.; Pople, J. A. *J. Chem. Phys.* **1993**, *98*, 5612.

(27) Felice, R. D.; Northrup, J. E. *Phys. Rev. B* **1999**, *60*, R16278.

(28) Wang, X. G.; Chaka, A.; Scheffler, M. *Phys. Rev. Lett.* **2000**, *84*, 3650.

(29) Tepesch, P. D.; Quong, A. A. *Phys. State Solid* (*B*) **2000**, *217*, 377.

(30) Siegel, D. J.; Hector, L. G., Jr.; Adams, J. B. *Phys. Rev. B* **2002**, ***65***, 085415.

(31) Verdozzi, C.; Jennison, D. R.; Schultz, P. A.; Sears, M. P. *Phys. Rev. Lett.* **1999**, *82*, 799.

(32) Felice, R. D.; Northrup, J. E. *Phys. Rev. B* **1999**, *60*, R16278.

(33) Peng, C.; Ayala, P. Y.; Schlegel, H. B.; Frisch, M. J. *J. Comput. Chem.* **1996**, *17*, 49.

(34) Peng, C.; Schlegel, H. B. *Isr. J. Chem.* **1994**, *33*, 449.

(35) Yang, R.; Wang, Y. M.; Ye H. Q.; Wang, C. Y. *J. Phys.*: *Condens. Matter* **2001**, *13*, 4485.

(36) Hong, T.; Smith, J. R.; Srolovitz, D. J. *J. Adhes. Sci. Technol.* **1994**, *8*, 837.

(37) Hong, T.; Smith, J. R.; Srolovitz, D. J. *Acta Metall. Mater.* **1995**, *43*, 2721.

(38) Gomes, J. R. B.; Illas, F.; Hernández, N. C.; Márquez, A.; Sanz, J. F. *Phys. Rev. B* **2002**, *65*, 125414.

(39) Nagy, L. T.; Micov, M.; Benco, L.; Liska, M.; Mach, P.; Tunega, D. *Int. J. Quantum Chem.* **1998**, *70*, 341.

(40) Yang, R.; Tanaka, S.; Kohyama, M. *Philos. Mag. Lett.* **2004**, *84*, 425.